CHAPTER

12 Cross-layer optimization for multihop cognitive radio networks

Yi Shi and Y. Thomas Hou
Virginia Polytechnic Institute and State University, United States

12.1 INTRODUCTION

From a wireless networking perspective, cognitive radio (CR) offers a whole new set of research problems in algorithm design and protocol implementation. To appreciate such opportunity, we compare CR with a closely related wireless networking technology called *multi-channel multi-radio* (MC-MR), which has also been under intensive research in recent years (see e.g., [534–538] and the references therein). First, MC-MR employs traditional hardware-based radio technology and hence each radio can operate on only a single channel at a time and there is no switching of channels on a per-packet basis. Therefore, the number of concurrent channels that can be used at a wireless node is limited by the number of radios. In contrast, the radio technology in a CR is software based; a software radio is capable of switching frequency bands on a per-packet basis. As a result, the number of concurrent frequency bands that can be used by a CR is typically much larger than that which can be supported by MC-MR. Second, a common assumption for MC-MR is that a set of "common channels" is available at every node in the network; each channel typically has the same bandwidth. Such assumption is hardly true for CR networks, in which each node may have a different set of available frequency bands, each of which may be of unequal size. A CR node is capable of working on a set of "heterogeneous" channels that are scattered over widely separated slices of the frequency spectrum with different bandwidths. An even more profound advance in CR technology is that CR can work on noncontiguous channels for transmission/reception. These important differences between MC-MR and CR warrant that algorithm design for future CR networks is substantially more complex than that

Doi: 10.1016/B978-0-12-374715-0.00012-5

for current MC-MR wireless networks. In some sense, an MC-MR wireless network can be considered a special case of CR network. Thus, algorithms designed for future CR networks can be tailored to address current MC-MR networks while the converse is not true.

Our goal is to optimize network-level performance of a multihop CR network. It is now well understood that network performance for such a network is tightly coupled with lower-layer behaviors [539]. For example, to determine the amount of flow that can be transported between two nodes, we need to compute this link's capacity under a particular power control and scheduling. Then we can determine how to fully utilize this link capacity by optimally assigning a flow rate on this link. For scheduling, before we decide if a link should be active on certain frequency bands, we should confirm that this link is indeed used in upper-layer routing. For those links that are not used in routing, we should not consider them for scheduling. For power control, before we determine transmission power at a node on a frequency band for a transmission, we should confirm that this transmission is indeed needed in routing and this band is indeed scheduled to be active on this node. Due to these interdependencies among the layers, a cross-layer design is essential to achieve optimal CR network performance.

Following a cross-layer optimization approach, in this chapter, we show how to jointly consider power control, scheduling, and routing at multiple layers (see Table 12.1). At the physical layer, we determine the transmission power at each CR node on each of its available frequency bands. We note that, although a larger transmission power can increase the transmission rate at this node, it also produces a larger interference at other nodes and may degrade the network performance. Therefore, we cannot simply set the transmission power to its maximum. We use the physical model [269] to characterize the power-rate relationship. Under the physical model, a transmission is successful if and only if the signal-to-interference-plus-noise-ratio (SINR) at the intended receiver exceeds a threshold so that the transmitted signal can be decoded with an acceptable bit error rate (BER). Further, capacity calculation is based on SINR (via Shannon's formula), which takes into account interference due to simultaneous transmission at other nodes. At the link layer, we arrange transmissions on different frequency bands such that each transmission has an SINR that exceeds a required threshold. We note that, although

Table 12.1 Mechanism Considered in This Chapter at Each Layer in the Protocol Stack

Layer in Protocol Stack	Mechanism Considered in This Chapter
Network layer	Multipath multihop flow routing
Link layer	Frequency scheduling
Physical layer	Per-node-based power control

activating multiple frequency bands on a link can increase the transmission rate on this link, it also produces interference to other nodes on the same band. Therefore, we need an optimal scheduling such that all transmission rates on all nodes can be maximized. At the network layer, we allow flow splitting and multihop routing to achieve the best performance. When we determine flow rates on each link, we need to consider the following two constraints. The first constraint is flow balance; that is, at each node (except the source and destination nodes) the total incoming data rates should be equal to the total outgoing data rates. The second constraint is link capacity constraint; that is, the total flow rates on each link cannot be more than the achievable capacity under power control and scheduling. We develop mathematical models for these complex relationships among power control, scheduling, and routing. These models are general and can be used for many related cross-layer problems for multihop CR networks.

As a case study, we apply our models to a specific cross-layer optimization problem. We consider how to maximize throughput capacity for CR networks. We assume there are multiple user communication sessions (source-destination pairs), each with a minimum rate requirement. We aim to maximize a common scaling factor of these minimum rate requirements via joint optimization of power control, scheduling, and routing. By applying our mathematical models, we formulate this problem as a mixed integer nonlinear program (MINLP). Although this problem is difficult to solve, we show how to develop a centralized solution to this complex optimization problem based on the so-called *branch-and-bound* (BB) framework and *reformulation-linearization technique* (RLT) [540]. The basic idea of branch and bound is divide and conquer. We apply this solution procedure on several network instances and show its efficacy.

We organize this chapter as follows. In Section 12.2, we present mathematical models for power control, scheduling, and routing. In Section 12.3, as a case study, we study the throughput maximization problem and give a solution based on the branch-and-bound framework. In Section 12.4, we present some numerical results for the proposed solution procedure. Section 12.5 concludes this chapter. Section 12.6 offers some problems as a review for this chapter.

12.2 MATHEMATICAL MODELS AT MULTIPLE LAYERS

We consider a CR-based ad hoc network with a set of nodes $\mathcal{N}$. For a node $i \in \mathcal{N}$, the set of available frequency bands $\mathcal{M}_i$ depends on its location and may not be identical to the available frequency bands at other nodes. We assume that the bandwidth of each frequency band (channel) is W. Denote by $\mathcal{M}$ the set of all frequency bands present in the network; that is, $\mathcal{M} = \bigcup_{i \in \mathcal{N}} \mathcal{M}_i$. Denote $\mathcal{M}_{ij} = \mathcal{M}_i \bigcap \mathcal{M}_j$, which is the set of frequency bands that is common on both nodes i and j and thus can be used for transmission between these two nodes. In the rest

of this section, we give mathematical models characterizing the interrelationships among different layers. Table 12.2 lists all notation in this chapter.

12.2.1 Scheduling and Power Control

In a multihop CR network, it is likely that there are multiple simultaneous transmissions in the network. On the same band, simultaneous transmission and reception are prohibited, as the transmission overwhelms the reception (also known as *self-interference*). For such self-interference, we must schedule transmission/reception either on different frequency bands or in different time slots. Also, within the network, transmissions at some nodes may interfere with other nonintended receiving nodes if they are on the same band and close to each other. Therefore, it is necessary to schedule the interfering transmission/reception either on a different band or in a different time slot.

Scheduling for transmission at each node in the network can be done either in the time domain or the frequency domain. In this chapter, we consider scheduling in the frequency domain in the form of assigning frequency bands (channels). Concurrent transmissions within the same channel are allowed as long as the interference level is acceptable.

Denote

$$x_{ij}^m = \begin{cases} 1 & \text{if node } i \text{ transmits data to node } j \text{ on band } m \\ 0 & \text{otherwise.} \end{cases} \tag{12.1}$$

To simplify the model, we assume that node i cannot use a band $m \in \mathcal{M}_i$ for transmitting different data to multiple nodes or for receiving different data from multiple nodes; that is,

$$\sum_{j \in \mathcal{T}_i^m} x_{ij}^m \leq 1, \tag{12.2}$$

$$\sum_{k \in \mathcal{T}_i^m} x_{ki}^m \leq 1, \tag{12.3}$$

where $\mathcal{T}_i^m$ is the set of nodes to which node i can transmit (and receive) on band m in the network. Further, due to self-interference, node i cannot use it for both transmission and reception; that is,

$$x_{ki}^m + x_{ij}^m \leq 1 (j, k \in \mathcal{T}_i^m, j \neq k). \tag{12.4}$$

Combining Equations (12.2), (12.3), and (12.4), we have

$$\sum_{k \in \mathcal{T}_i^m} x_{ki}^m + \sum_{j \in \mathcal{T}_i^m} x_{ij}^m \leq 1. \tag{12.5}$$

Figure 12.1 illustrates the scheduling constraint, where node i is receiving from node k and transmitting to nodes j and h. Then, by Equation (12.5), node i needs to use three different bands for these transmissions/receptions.

Table 12.2 Notation Used in This Chapter

Symbol	Definition
$\mathcal{N}$	The set of nodes in the network
$\mathcal{M}_i$	The set of available bands at node $i \in \mathcal{N}$
$\mathcal{M}$	The set of frequency bands in the network, $\mathcal{M} = \sum_{i \in \mathcal{N}} \mathcal{M}_i$
$\mathcal{M}_{ij}$	The set of available bands on link $i \rightarrow j$, $\mathcal{M}_{ij} = \mathcal{M}_i \bigcap \mathcal{M}_j$
W	Bandwidth of a frequency band
$\mathcal{L}$	The set of active user communication sessions in the network
$s(l)$, $d(l)$	Source and destination nodes of session $l \in \mathcal{L}$
$r(l)$	Minimum rate requirement of session l
K	Rate scaling factor for all sessions
$P_{\max}$	The maximum transmission power at a transmitter
η	Ambient Gaussian noise density
g_{ij}	Propagation gain from node i to node j
α	The minimum required SINR
$\mathcal{T}_i^m$	The set of nodes that node i can transmit to (and receive from) on band m
$\mathcal{T}_i$	The set of nodes that node i can transmit to (and receive from) $\mathcal{T}_i = \bigcup_{m \in \mathcal{M}_i} \mathcal{T}_i^m$
$\mathcal{I}_j^m$	The set of nodes that may produce interference on band m at node j
x_{ij}^m	Binary indicator to mark whether or not band m is used by link $i \rightarrow j$
$f_{ij}(l)$	Data rate attributed to session l on link $i \rightarrow j$
Q	The number of transmission power levels at a transmitter
q_{ij}^m	The transmission power level from node i to node j on band m
t_i^m	The transmission power level at node i on band m, $t_i^m = \sum_{j \in \mathcal{T}_i^m} q_{ij}^m$
s_{ij}^m	The SINR from node i to node j on band m
ε	A small positive constant reflecting the desired accuracy
Ω_z	The set of all possible values of $(\mathbf{x}, \mathbf{q})$ in problem z
LB_z, UB_z	The lower and upper bounds of problem z
ψ_z	The solution obtained by local search for problem z
LB, UB	The minimum lower and upper bounds among all problems
ψ_ε	A $(1 - \varepsilon)$ optimal solution

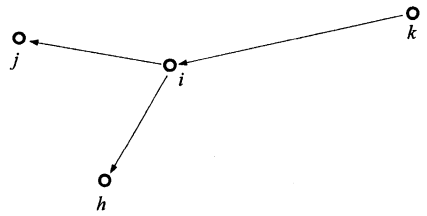

FIGURE 12.1

An example of scheduling constraint at node i. Each transmission/receiption at node i needs a different band.

Now we consider power control and its relationship with scheduling. At each CR node, the node's transmission power on each band is bounded by $P_{\max}$. Since the interference from this link to other links depends on transmission power, it is necessary to determine the optimal transmission power for each node on each band.

For power control, it is reasonable to assume that the transmission power at a node is limited to a finite number of discrete levels between 0 and $P_{\max}$. To model this discrete power control mathematically, we introduce an integer parameter Q that represents the total number of power levels to which a transmitter can be adjusted; that is, $0, \frac{1}{Q}P_{\max}, \frac{2}{Q}P_{\max}, \ldots, P_{\max}$. Denote $q_{ij}^m \in \{0, 1, 2, \ldots, Q\}$ the integer power level. Clearly, when node i does not transmit data to node j on band m, q_{ij}^m is 0. Under the maximum allowed transmission power level Q, we have

$$q_{ij}^m \begin{cases} \leq Q & \text{if } x_{ij}^m = 1 \\ = 0 & \text{otherwise.} \end{cases}$$

With joint consideration of x_{ij}^m and q_{ij}^m, this relationship can be rewritten as

$$q_{ij}^m \leq Q x_{ij}^m. \tag{12.6}$$

As discussed earlier, concurrent transmissions by different nodes on the same band are allowed as long as the interference level is kept under control. Under the physical model [269], a transmission is successful if and only if the SINR at the receiving node exceeds a certain threshold, say α. We now formulate this constraint. For a transmission from node i to node j on band m, when there is interference from concurrent transmissions on the same band, the SINR at node j (denoted as s_{ij}^m) is

$$s_{ij}^m = \frac{g_{ij}\frac{q_{ij}^m}{Q}P_{\max}}{\eta W + \sum_{k\in\mathcal{N}}^{k\neq i,j}\sum_{b\in\mathcal{T}_k^m}^{b\neq i,j} g_{kj}\frac{q_{kb}^m}{Q}P_{\max}} = \frac{g_{ij}q_{ij}^m}{\frac{\eta WQ}{P_{\max}} + \sum_{k\in\mathcal{N}}^{k\neq i,j}\sum_{b\in\mathcal{T}_k^m}^{b\neq i,j} g_{kj}q_{kb}^m},$$

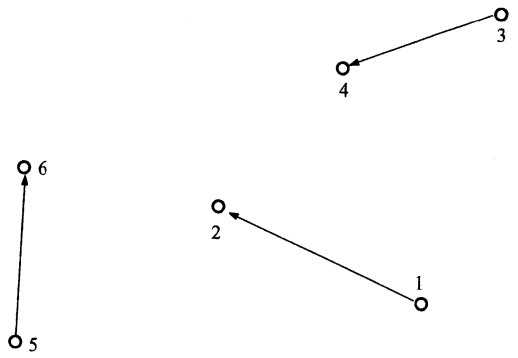

FIGURE 12.2

Three simultaneous transmissions on the same frequency band. At receiving node 2, transmissions from nodes 3 and 5 are considered interference, as node 2 is not the intended receiver for these transmissions.

where η is the ambient Gaussian noise density and g_{ij} is the propagation gain from node i to node j. As an example, suppose three transmissions, $1 \to 2$, $3 \to 4$, and $5 \to 6$, are on band m at the same time (see Figure 12.2). At node 2, there is interference from nodes 3 and 5. Therefore, the SINR at node 2 is

$$s_{12}^m = \frac{g_{12}q_{12}^m}{\frac{\eta WQ}{P_{\max}} + g_{31}q_{34}^m + g_{51}q_{56}^m}.$$

To get a more compact constraint, note that, when there is a transmission from node i to node j on band m, we have $x_{ij}^m = 1$. Then, by Equation (12.5), $x_{ki}^m = 0$ for $k \in \mathcal{T}_i^m$ and $x_{kj}^m = 0$ for $k \in \mathcal{T}_j^m$. Hence, by Equation (12.6), $q_{ki}^m = 0$ and $q_{kj}^m = 0$. Then we have

$$s_{ij}^m = \frac{g_{ij}q_{ij}^m}{\frac{\eta WQ}{P_{\max}} + \sum_{k\in\mathcal{N}}^{k\neq i,j}\sum_{b\in\mathcal{T}_k^m} g_{kj}q_{kb}^m}.$$

Denote $t_k^m = \sum_{b\in\mathcal{T}_k^m} q_{kb}^m$. We have

$$s_{ij}^m = \frac{g_{ij}q_{ij}^m}{\frac{\eta WQ}{P_{\max}} + \sum_{k\in\mathcal{N}}^{k\neq i,j} g_{kj}t_k^m}. \tag{12.7}$$

Note that this SINR computation also holds when $q_{ij}^m = 0$; that is, when there is no transmission from node i to node j on band m.

Recall that, under the physical model, a transmission from node i to node j on band m is successful if and only if the SINR at node j exceeds a threshold α; that is, $s_{ij}^m \geq \alpha$. This is the necessary and sufficient condition for successful transmission

under the physical model. Then, by Equation (12.1), we have

$$x_{ij}^m = \begin{cases} 1 & \text{if } s_{ij}^m \geq \alpha \\ 0 & \text{otherwise.} \end{cases}$$

This can be written into the following compact inequality:

$$s_{ij}^m \geq \alpha x_{ij}^m.$$

12.2.2 Routing

In an ad hoc network, consider a set of $\mathcal{L}$ active user communication (unicast) sessions. Denote by $s(l)$ and $d(l)$ the source and destination nodes of session $l \in \mathcal{L}$ and $r(l)$ the minimum rate requirement (in bits/second) of session l. To route these flows from their respective source nodes to destination nodes, it is necessary to employ multihop due to the limited transmission range of a node. Further, to have more flexibility, it is desirable to allow flow splitting and multipath routing. That is, the data flow from a source can be split into subflows and each subflow can traverse different paths to the flow's destination. This is because a single path is overly restrictive and may not yield an optimal solution. In routing constraints, we need to ensure that flow balance holds at each node (except source and destination nodes).

In the case study in Section 12.3, we consider how to maximize a rate scaling factor K for all session rates. That is, for each session $l \in \mathcal{L}$, $r(l)K$ amount of data rate is to be sent from $s(l)$ to $d(l)$. In this context, the routing constraints can be modeled as follows.

Denote by $f_{ij}(l)$ the data rate on link (i,j) attributed to session l, where $i \in \mathcal{N}, j \in \mathcal{T}_i = \bigcup_{m \in \mathcal{M}_i} \mathcal{T}_i^m$. If node i is the source node of session l—that is, $i = s(l)$—then flow balance at node i must hold. That is,

$$\sum_{j \in \mathcal{T}_i} f_{ij}(l) = r(l)K. \tag{12.8}$$

If node i is an intermediate relay node for session l—that is, $i \neq s(l)$ and $i \neq d(l)$—then

$$\sum_{\substack{j \in \mathcal{T}_i \\ j \neq s(l)}} f_{ij}(l) = \sum_{\substack{k \in \mathcal{T}_i \\ k \neq d(l)}} f_{ki}(l). \tag{12.9}$$

If node i is the destination node of session l—that is, $i = d(l)$—then

$$\sum_{k \in \mathcal{T}_i} f_{ki}(l) = r(l)K. \tag{12.10}$$

It can be easily verified that, once Equations (12.8) and (12.9) are satisfied, Equation (12.10) is also satisfied. As a result, it is sufficient to list only Equations (12.8) and (12.9) in the formulation.

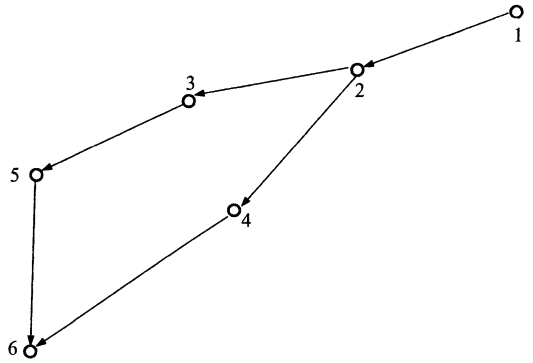

FIGURE 12.3

Multipath routing for a session l with $s(l) = 1$ and $d(l) = 6$.

An example of multipath routing for a session l is shown in Figure 12.3, where node 1 is the source and node 6 is the destination. At the source node 1, we have

$$f_{12}(l) = r(l)K. \tag{12.11}$$

At intermediate relay node 2, the data received from node 1 are split into two flows, and we have

$$f_{23}(l) + f_{24}(l) = f_{12}(l). \tag{12.12}$$

At intermediate relay node 3, the data received from node 2 are sent to node 5, and we have

$$f_{35}(l) = f_{23}(l). \tag{12.13}$$

Similarly, we have the following constraints at nodes 4 and 5:

$$f_{46}(l) = f_{24}(l), \tag{12.14}$$

$$f_{56}(l) = f_{35}(l). \tag{12.15}$$

At destination 6, we have

$$f_{46}(l) + f_{56}(l) = r(l)K. \tag{12.16}$$

Note that, by taking the sum of the left and right sides in Equations (12.11), (12.12), (12.13), (12.14), and (12.15), we have

$$\begin{aligned} &f_{12}(l) + [f_{23}(l) + f_{24}(l)] + f_{35}(l) + f_{46}(l) + f_{56}(l) \\ &= r(l)K + f_{12}(l) + f_{23}(l) + f_{24}(l) + f_{35}(l). \end{aligned}$$

After cancelation of common terms on both sides, we have

$$f_{46}(l) + f_{56}(l) = r(l)K,$$

which is precisely Equation (12.16). Therefore, it is not necessary to include the flow constraint at destination nodes (i.e., Equation (12.10)) once we have Equation (12.8) at source nodes and Equation (12.9) at relay nodes.

In addition to these flow constraints at each node $i \in \mathcal{N}$ for session $l \in \mathcal{L}$, the aggregated flow rates on each radio link cannot exceed that link's capacity. That is, on a link $i \to j$, we must have

$$\sum_{l \in \mathcal{L}}^{s(l)\neq j, d(l)\neq i} f_{ij}(l) \le \sum_{m \in \mathcal{M}_{ij}} W \log_2(1 + s_{ij}^m). \tag{12.17}$$

The constraint in Equation (12.17) illustrates the coupling relationship among flow routing (via $f_{ij}(l)$), power control (embedded in s_{ij}^m), and scheduling (embedded in s_{ij}^m).

12.3 A CASE STUDY: THE THROUGHPUT MAXIMIZATION PROBLEM

As a case study, we study the throughput maximization problem for a multihop CR network. We consider multihop, multipath routing to transmit data from each source to their corresponding destination. We show how to maximize a rate scaling factor K for all active sessions. That is, for each active session $l \in \mathcal{L}$, what is the maximum K we can have while $r(l)K$ amount of data rate can be transmitted from $s(l)$ to $d(l)$?

12.3.1 Problem Formulation

By applying the mathematical models in Section 12.2 and putting together all the constraints for scheduling, power control, and flow routing, we have the following mathematical formulation:

$$\text{Max} \quad K \tag{12.18}$$

$$\text{s.t.} \quad \sum_{i \in \mathcal{T}_k^m} x_{ki}^m + \sum_{j \in \mathcal{T}_i^m} x_{ij}^m \le 1 \quad (i \in \mathcal{N}, m \in \mathcal{M}_i)$$

$$q_{ij}^m - Q x_{ij}^m \le 0 \quad (i \in \mathcal{N}, m \in \mathcal{M}_i, j \in \mathcal{T}_i^m) \tag{12.19}$$

$$\sum_{j \in \mathcal{T}_i^m} q_{ij}^m - t_i^m = 0 \quad (i \in \mathcal{N}, m \in \mathcal{M}_i) \tag{12.20}$$

$$\frac{\eta W Q}{P_{\max}} s_{ij}^m + \sum_{k \in \mathcal{N}}^{k \neq i,j} g_{kj} t_k^m s_{ij}^m - g_{ij} q_{ij}^m = 0 \quad (i \in \mathcal{N}, m \in \mathcal{M}_i, j \in \mathcal{T}_i^m) \tag{12.21}$$

$$\alpha x_{ij}^m - s_{ij}^m \le 0 \quad (i \in \mathcal{N}, m \in \mathcal{M}_i, j \in \mathcal{T}_i^m) \tag{12.22}$$

$$\sum_{l \in \mathcal{L}}^{s(l)\neq j, d(l)\neq i} f_{ij}(l) - \sum_{m \in \mathcal{M}_{ij}} W \log_2(1 + s_{ij}^m) \le 0 \quad (i \in \mathcal{N}, j \in \mathcal{T}_i)$$

$$\sum_{j \in \mathcal{T}_i} f_{ij}(l) - r(l)K = 0 \quad (l \in \mathcal{L}, i = s(l))$$

$$\sum_{j \in \mathcal{T}_i}^{j \neq s(l)} f_{ij}(l) - \sum_{i \in \mathcal{T}_k}^{k \neq d(l)} f_{ki}(l) = 0 \quad (l \in \mathcal{L}, i \in \mathcal{N}, i \neq s(l), d(l))$$

$$x_{ij}^m \in \{0,1\}, q_{ij}^m \in \{0,1,2,\cdots,Q\}, t_i^m, s_{ij}^m \ge 0 \quad (i \in \mathcal{N}, m \in \mathcal{M}_i, j \in \mathcal{T}_i^m)$$

$$K, f_{ij}(l) \ge 0 \quad (l \in \mathcal{L}, i \in \mathcal{N}, i \neq d(l), j \in \mathcal{T}_i, j \neq s(l)),$$

where $Q, \eta, W, \alpha, P_{\max}, g_{ij}$, and $r(l)$ are all constants and $K, x_{ij}^m, q_{ij}^m, t_i^m, s_{ij}^m$, and $f_{ij}(l)$ are all optimization variables. This formulation is a mixed-integer nonlinear program, which is NP-hard in general [541].

12.3.2 Solution Overview

For the complex MINLP problem, we employ the so-called *branch-and-bound* framework [542] to develop a solution. Under branch and bound, we aim to provide a $(1 - \varepsilon)$ optimal solution, where ε is a small positive constant reflecting our desired accuracy in the final solution.

Initially, branch and bound analyzes the value sets for each partition variable; that is, all discrete variables and all variables in a nonlinear term. For our problem, these variables include all $x_{ij}^m, q_{ij}^m, t_i^m$, and s_{ij}^m variables. The value sets for each partition variable are $x_{ij}^m \in \{0,1\}, q_{ij}^m \in \{0,1,2,\ldots,Q\}, t_i^m \in \{0,1,2,\ldots,Q\}$, and $s_{ij}^m \in [0, g_{ij}P_{\max}/\eta W]$. By using some *relaxation* techniques—that is, replacing a discrete variable by a continuous variable and replacing a nonlinear constraint by several linear constraints—branch and bound obtains a linear relaxation for the original problem based on the value sets for each partition variable. The solution to this relaxed problem provides an upper bound (UB) to the objective function. As we shall show shortly, this critical step is made possible by the convex hull relaxation for nonlinear discrete terms. We call the approximation errors caused by relaxation *relaxation errors*. Due to these relaxation errors, the solution to the relaxed problem usually is infeasible to the original problem. To obtain a feasible solution to the original problem, branch and bound uses a *local search* algorithm and the relaxation solution as the starting point. The obtained feasible solution provides a lower bound (LB) for the objective function (see Figure 12.4(a) for an example). If the obtained lower and upper bounds are close to each other within

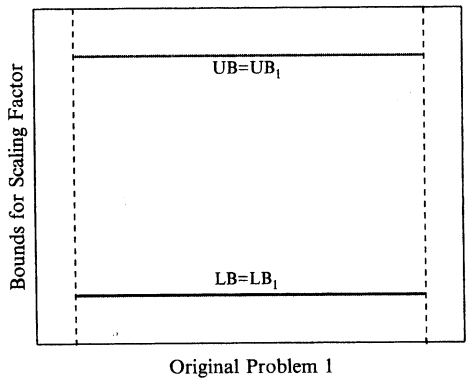

(a) Iteration 1. We can estimate UB and LB for the original problem.

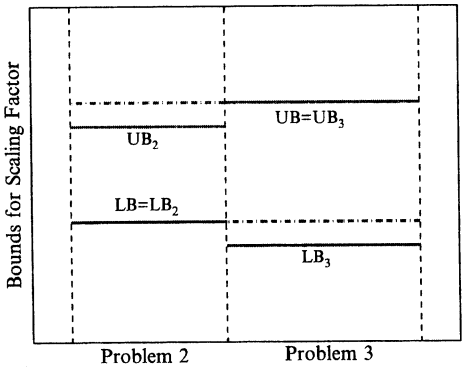

(b) Iteration 2. By dividing the original problem into two new problems, we can develop tighter bounds on each problem (UB_2, LB_2 for Problem 2 and UB_3, LB_3 for Problem 3). Thus, bounds ($UB = UB_3$ and $LB = LB_2$) for the original problem also become tighter.

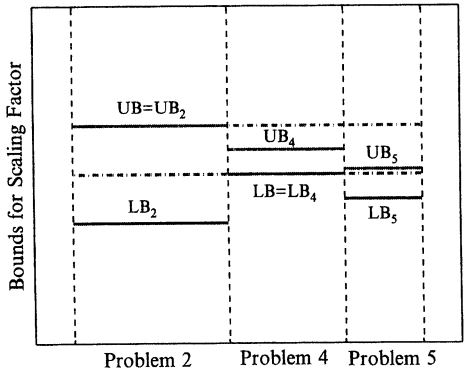

(c) Iteration 3. By dividing Problem 3 (with the largest upper bound) into two new problems, we can obtain tighter upper and lower bounds to Problem 3. Thus, bounds for the original problem can be further improved as $UB = UB_2$ and $LB = LB_4$.

FIGURE 12.4

Illustration of branch and bound solution procedure

a factor of ε—that is, $LB \geq (1-\varepsilon)UB$—then the current feasible solution is $(1-\varepsilon)$ optimal and we are done.

If the relaxation errors for nonlinear terms are not small, then the gap between the upper bound UB and the lower bound LB could be large. To close this gap, we must have a tighter linear relaxation; that is, with smaller relaxation errors. This could be achieved by further narrowing down the value sets of partition variables. Specifically, branch and bound selects a partition variable with the maximum relaxation error and divides its value set into two sets by its value in the relaxation solution. Then the original Problem 1 is divided into two new Problems 2 and 3 (see Figure 12.4(b)). Again, branch and bound performs relaxation and local search on these two new problems. Now we have upper bounds UB_2 and UB_3 for Problems 2 and 3, respectively. We also have feasible solutions that provide lower bounds LB_2 and LB_3 for Problems 2 and 3, respectively. Since the relaxations in Problems 2 and 3 are both tighter than in Problem 1, we have $\max\{UB_2, UB_3\} \leq UB_1$ and $\max\{LB_2, LB_3\} \geq LB_1$. For a maximization problem, the upper bound of the original problem is updated from $UB = UB_1$ to $UB = \max\{UB_2, UB_3\}$. Also, the best feasible solution to the original problem is the solution with a larger LB_i. Then the lower bound of the original problem is updated from $LB = LB_1$ to $LB = \max\{LB_2, LB_3\}$. As a result, we now have a smaller gap between UB and LB. Then we either have a $(1-\varepsilon)$-optimal solution (if $LB \geq (1-\varepsilon)\,UB$), or choose a problem with the maximum upper bound (Problem 3 in Figure 12.4(b)), and perform partition on this problem.

An important property of branch and bound is that we may remove some problems from further consideration before we solve it completely. During the iteration process for branch and bound, if we find a Problem z with $LB \geq (1-\varepsilon)UB_z$, then we conclude that this problem cannot provide much improvement on LB, see Problem 4 in Figure 12.4(c). That is, further branching on this problem will not yield much improvement so we can remove this problem from further consideration.

It has been shown that, under very general conditions, a branch-and-bound solution procedure always converges [540]. Although the worst-case complexity of such a procedure is exponential, the actual running time, based on our experience, is reasonably fast if all partition variables are discrete variables (e.g., the problem considered in our case study).

Figure 12.5 shows the general framework of the branch-and-bound procedure. Note that the key components in the branch-and-bound framework are problem specific and must be carefully designed to make it work. These include (1) how to obtain a linear relaxation, (2) how to perform a local search, and (3) how to choose a variable for partition. The details of these components are presented in Sections 12.3.3, 12.3.4, and 12.3.5, respectively.

12.3.3 Linear Relaxation

During each iteration of the branch-and-bound procedure, we need a linear relaxation technique to obtain an upper bound on the objective function (see line 5 in Figure 12.5).

Branch-and-Bound Procedure

1. Initialization:
2. Let the initial best solution $\psi_\varepsilon = \emptyset$ and the initial lower bound LB $= -\infty$.
3. Determine initial value set for each partition variable.
4. Let the initial problem list include only the original problem, denoted as Problem 1.
5. Build a linear relaxation and obtain the relaxation solution $\hat{\psi}_1$.
6. The objective value of $\hat{\psi}_1$ is an upper bound UB_1 to Problem 1.
7. Iteration:
8. Select Problem z that has the maximal UB_z among all problems in the problem list.
9. Update upper bound UB $= UB_z$.
10. Find a feasible solution ψ_z from $\hat{\psi}_z$ via a local search algorithm and denote its objective value as LB_z.
11. If ($LB_z >$ LB) {
12. Update $\psi_\varepsilon = \psi_z$ and LB $= LB_z$.
13. If LB $\geq (1-\varepsilon)$UB, we stop with the $(1-\varepsilon)$ optimal solution ψ_ε.
14. Otherwise, remove all Problems z' with LB $\geq (1-\varepsilon)UB_{z'}$ from the problem list. }
15. Select a variable with the maximum relaxation error and divide its value set into two sets by its value in $\hat{\psi}_z$.
16. Create two new Problems z_1 and z_2 based on these two sets.
17. Remove Problem z from the problem list.
18. Obtain UB_{z1} and UB_{z2} for Problems z_1 and z_2 via their linear relaxations.
19. If LB $< (1-\varepsilon)UB_{z1}$, add Problem z_1 into the problem list.
20. If LB $< (1-\varepsilon)UB_{z2}$, add Problem z_2 into the problem list.
21. If the problem list is empty, we stop with a $(1-\varepsilon)$ optimal solution ψ_ε.
22. Otherwise, go to the next iteration.

FIGURE 12.5

Pseudocode for the branch-and-bound solution procedure.

For the polynomial term $t_k^m s_{ij}^m$ in the problem formulation, we can apply a method called *reformulation-linearization technique* [540]. For a nonlinear term $t_k^m s_{ij}^m$, we introduce a new variable u_{ijk}^m; replace $t_k^m s_{ij}^m$ with u_{ijk}^m; and add RLT constraints on these variables. Suppose t_k^m and s_{ij}^m are bounded by $(t_k^m)_L \leq t_k^m \leq (t_k^m)_U$ and $(s_{ij}^m)_L \leq s_{ij}^m \leq (s_{ij}^m)_U$, respectively. Hence, we have $[t_k^m - (t_k^m)_L] \cdot [s_{ij}^m - (s_{ij}^m)_L] \geq 0$, $[t_k^m - (t_K^m)_L] \cdot [(s_{ij}^m)_U - s_{ij}^m] \geq 0$, $[(t_k^m)_U - t_k^m] \cdot [s_{ij}^m - (s_{ij}^m)_L] \geq 0$, and $[(t_k^m)_U - t_k^m] \cdot [(s_{ij}^m)_U - s_{ij}^m] \geq 0$. From these relationships and substituting $u_{ijk}^m = t_k^m s_{ij}^m$, we have the following RLT constraints for u_{ijk}^m:

$$(t_k^m)_L \cdot s_{ij}^m + (s_{ij}^m)_L \cdot t_k^m - u_{ijk}^m \leq (t_k^m)_L \cdot (s_{ij}^m)_L,$$
$$(t_k^m)_U \cdot s_{ij}^m + (s_{ij}^m)_L \cdot t_k^m - u_{ijk}^m \geq (t_k^m)_U \cdot (s_{ij}^m)_L,$$
$$(t_k^m)_L \cdot s_{ij}^m + (s_{ij}^m)_U \cdot t_k^m - u_{ijk}^m \geq (t_k^m)_L \cdot (s_{ij}^m)_U,$$
$$(t_k^m)_U \cdot s_{ij}^m + (s_{ij}^m)_U \cdot t_k^m - u_{ijk}^m \leq (t_k^m)_U \cdot (s_{ij}^m)_U.$$

For the log term, we propose to employ three tangential supports as an approximation (see Figure 12.6). These three tangential segments form a convex hull linear relaxation. We first analyze the bounds for $1 + s_{ij}^m$. Then, we introduce a variable

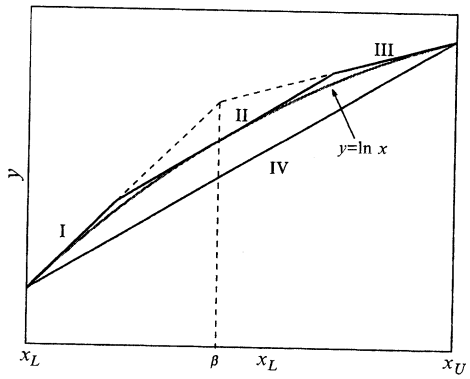

FIGURE 12.6

A convex hull for $y = \ln x$ to obtain its linear relaxation, where segments I, II, and III define upper bounds and segment IV defines a lower bound.

$c_{ij}^m = \ln(1 + s_{ij}^m)$ and consider how to get a linear relaxation for $y = \ln x$ over $x_L \leq x \leq x_U$. This function can be bounded by four segments (or a convex hull), where segments I, II, and III are tangential supports and segment IV is the chord (see Figure 12.6). In particular, three tangent segments are at $(x_L, \ln x_L)$, $(\beta, \ln \beta)$, and $(x_U, \ln x_U)$, where $\beta = [x_L \cdot x_U \cdot (\ln x_U - \ln x_L)]/(x_U - x_L)$ is the horizontal location for the point intersects extended tangent segments I and III; segment IV is the segment that joins points $(x_L, \ln x_L)$ and $(x_U, \ln x_U)$. The convex region defined by the four segments can be described by the following four linear constraints:

$$x_L \cdot y - x \leq x_L(\ln x_L - 1),$$
$$\beta \cdot y - x \leq \beta(\ln \beta - 1),$$
$$x_U \cdot y - x \leq x_U(\ln x_U - 1),$$
$$(x_U - x_L)y + (\ln x_L - \ln x_U)x \geq x_U \cdot \ln x_L - x_L \cdot \ln x_U.$$

As a result, the non-polynomial (log) term can also be relaxed into linear constraints.

Denote $\mathbf{x}$, $\mathbf{q}$, $\mathbf{t}$, and $\mathbf{s}$ as the vectors for variables x_{ij}^m, q_{ij}^m, t_i^m, and s_{ij}^m, respectively. We have the following linear relaxation for Problem z:

$$\text{Max} \quad K$$

$$\text{subject to} \quad \sum_{i \in \mathcal{T}_k^m} x_{ki}^m + \sum_{j \in \mathcal{T}_i^m} x_{ij}^m \leq 1 \qquad (i \in \mathcal{N}, m \in \mathcal{M}_i)$$

$$q_{ij}^m - Q x_{ij}^m \leq 0 \qquad (i \in \mathcal{N}, m \in \mathcal{M}_i, j \in \mathcal{T}_i^m) \quad (12.23)$$

$$\sum_{j \in \mathcal{T}_i^m} q_{ij}^m - t_i^m = 0 \qquad (i \in \mathcal{N}, m \in \mathcal{M}_i)$$

$$\frac{\eta WQ}{P_{\max}} s_{ij}^m + \sum_{k\in\mathcal{N}}^{k\neq i,j} g_{kj} u_{ijk}^m - g_{ij} q_{ij}^m = 0 \quad (i \in \mathcal{N}, m \in \mathcal{M}_i, j \in \mathcal{T}_i^m)$$

$$\text{RLT constraints for } u_{ijk}^m \quad (i,k \in \mathcal{N}, m \in \mathcal{M}_i, j \in \mathcal{T}_i^m, k \neq i,j)$$

$$\alpha x_{ij}^m - s_{ij}^m \leq 0 \quad (i \in \mathcal{N}, m \in \mathcal{M}_i, j \in \mathcal{T}_i^m)$$

$$\sum_{l\in\mathcal{L}}^{s(l)\neq j, d(l)\neq i} f_{ij}(l) - \sum_{m\in\mathcal{M}_{ij}} \frac{W}{\ln 2} c_{ij}^m \leq 0 \quad (i \in \mathcal{N}, j \in \mathcal{T}_i)$$

$$\text{Convex hull constraints for } c_{ij}^m \quad (i \in \mathcal{N}, m \in \mathcal{M}_i, j \in \mathcal{T}_i^m)$$

$$\sum_{j\in\mathcal{T}_i} f_{ij}(l) - r(l)K = 0 \quad (l \in \mathcal{L}, i = s(l))$$

$$\sum_{j\in\mathcal{T}_i}^{j\neq s(l)} f_{ij}(l) - \sum_{i\in\mathcal{T}_k}^{k\neq d(l)} f_{ki}(l) = 0 \quad (l \in \mathcal{L}, i \in \mathcal{N}, i \neq s(l), d(l))$$

$$c_{ij}^m, u_{ijk}^m \geq 0 \quad (i,k \in \mathcal{N}, m \in \mathcal{M}_i, j \in \mathcal{T}_i^m, k \neq i,j)$$

$$K, f_{ij}(l) \geq 0 \quad (l \in \mathcal{L}, i \in \mathcal{N}, i \neq d(l), j \in \mathcal{T}_i, j \neq s(l))$$

$$(\mathbf{x}, \mathbf{q}, \mathbf{t}, \mathbf{s}) \in \Omega_z,$$

where Ω_z is defined as $\Omega_z = \{(\mathbf{x}, \mathbf{q}, \mathbf{t}, \mathbf{s}) : (x_{ij}^m)_L \leq x_{ij}^m \leq (x_{ij}^m)_U, (q_{ij}^m)_L \leq q_{ij}^m \leq (q_{ij}^m)_U, (t_i^m)_L \leq t_i^m \leq (t_i^m)_U, (s_{ij}^m)_L \leq s_{ij}^m \leq (s_{ij}^m)_U\}$, which is the set of all possible values of $(\mathbf{x}, \mathbf{q}, \mathbf{t}, \mathbf{s})$ in Problem z, where $(x_{ij}^m)_L, (x_{ij}^m)_U, (q_{ij}^m)_L, (q_{ij}^m)_U, (s_{ij}^m)_L$, and $(s_{ij}^m)_U$ are constant bounds. For example, Ω_1 for the original Problem 1 is $\{(\mathbf{x}, \mathbf{q}, \mathbf{t}, \mathbf{s}) : 0 \leq x_{ij}^m \leq 1, 0 \leq q_{ij}^m \leq Q, 0 \leq t_i^m \leq Q, 0 \leq s_{ij}^m \leq \frac{g_{ij}P_{\max}}{\eta W}\}$.

12.3.4 Local Search Algorithm

A linear relaxation for a Problem z as discussed in Equation (12.23) can be solved in polynomial time. Denote the relaxation solution as $\hat{\psi}_z$, which provides an upper bound to Problem z but may not be feasible to the original problem (12.18) due to relaxation errors. We now show how to obtain a feasible solution ψ_z to the original problem based on relaxed solution $\hat{\psi}_z$ (see line 10 in Figure 12.5).

To obtain a feasible solution, we need to determine the integer values for $\mathbf{x}$ and $\mathbf{q}$ in solution ψ_z such that Equations (12.5), (12.19), and (12.22) hold. All other variables are based on $\mathbf{x}, \mathbf{q}$. Initially, each q_{ij}^m is set to the smallest value $(q_{ij}^m)_L$ in its value set and x_{ij}^m is fixed to 0 or 1 if its value set has only one element 0 or 1, respectively. Based on these values of q_{ij}^m, we can compute the capacity $\sum_{m\in\mathcal{M}_{ij}} W \cdot \log_2\left[1 + g_{ij}q_{ij}^m/(\eta WQ/P_{\max} + \sum_{k\in\mathcal{N}}^{k\neq i,j} g_{kj}t_k^m)\right]$ for each link $i \to j$. The requirement on a link $i \to j$ is $\sum_{l\in\mathcal{L}}^{s(l)\neq j, d(l)\neq i} \hat{f}_{ij}(l)$. Thus, we can compute k_{ij}, the ratio between the capacity and the requirement. The objective value for the current $\mathbf{x}$ and $\mathbf{q}$ is $K \cdot \min\{k_{ij} : i \in \mathcal{N}, j \in \mathcal{T}_i\}$. Therefore, we aim to increase the minimum k_{ij}. For the link with the smallest k_{ij}, we try to increase some q_{ij}^m under the constraint of $q_{ij}^m \leq (q_{ij}^m)_U$. When we cannot further increase the smallest k_{ij}, we are done. The details of this local search algorithm are shown in Figure 12.7.

Local Search Algorithm

1. Initialization:
2. Set $q_{ij}^m = (q_{ij}^m)_L$ and x_{ij}^m as 0 or 1 if its value set only has one element 0 or 1, respectively.
3. Compute the requirement $\sum_{l\in\mathcal{L}}^{s(l)\neq j, d(l)\neq i} \hat{f}_{ij}(l)$.
4. Iteration:
5. Compute capacity $\sum_{m\in\mathcal{M}_{ij}} W \log_2\left(1 + \frac{g_{ij}q_{ij}^m}{\eta WQ/P_{\max} + \sum_{k\in\mathcal{N}}^{k\neq i,j} g_{kj}t_k^m}\right)$ and the ratio k_{ij} between the capacity and the requirement for each link $i \to j$.
6. Suppose link $i \to j$ has the smallest k_{ij}. Try to increase its capacity as follows.
7. If q_{ij}^m can be increased on an already used band {
8. Suppose band m has the largest $\hat{q}_{ij}^m$ among these bands.
9. Increase q_{ij}^m under the constraints of $q_{ij}^m \leq (q_{ij}^m)_U$ and the corresponding $k_{ij} \leq 1$. }
10. else, if q_{ij}^m can be increased on an available but currently unused band {
11. Suppose band m has the largest $\hat{q}_{ij}^m$ among these bands.
12. Increase q_{ij}^m under the constraints of $q_{ij}^m \leq (q_{ij}^m)_U$ and the corresponding $k_{ij} \leq 1$.
13. Set $x_{ij}^m = 1, x_{ib}^m = 0$ for $b \in \mathcal{T}_i, b \neq j, x_{ki}^m = 0$ for $k \in \mathcal{T}_i$. }
14. else the iteration terminates.

FIGURE 12.7

Pseudocode of a local search algorithm to find a feasible solution.

12.3.5 Selection of Partition Variables

If the relaxation error for a Problem z is not small, the gap between its lower and upper bounds may be large. To obtain a small gap, we generate two new subproblems z_1 and z_2 from Problem z. We hope that these two new problems will have smaller relaxation errors. Then the bounds for them can be tighter than the bounds for z. Therefore, we identify a variable based on its relaxation error in line 15, Figure 12.5.

Note that the choice of a partition variable affects the convergence speed. Here, the candidate variables for partitioning are based on their impacts on the objective value, variables in $\mathbf{x}$ are more significant than variables in $\mathbf{q}$. Hence, we should first select one of $\mathbf{x}$ variables as the branch variable. In particular, for the relaxation solution $\hat{\psi}_z$, the relaxation error of a discrete variable x_{ij}^m is $\min\{\hat{x}_{ij}^m, 1 - \hat{x}_{ij}^m\}$, where $\hat{x}_{ij}^m$ is the value of variable x_{ij}^m in solution $\hat{\psi}_z$. We choose an x_{ij}^m with the maximum relaxation error among all $\mathbf{x}$ variables and set its value to $\{0\}$ and $\{1\}$ in Problems z_1 and z_2, respectively. Since the value set for this x_{ij}^m has only one element, this x_{ij}^m can be replaced by a constant in the new problem. As a result, some constraints may also be removed.

It should be noted that we may pose more limitations on other variables based on the new value set of x_{ij}^m. That is, if x_{ij}^m is 0, then we have $q_{ij}^m = 0$ based on Equation (12.19). If x_{ij}^m is 1, then we have $x_{ib}^m = 0$ for $b \in \mathcal{T}_i, b \neq j$ and $x_{ki}^m = 0$ for $k \in \mathcal{T}_i$ based on Equation (12.5).

When none of the $\mathbf{x}$ variables can be partitioned (i.e., all x variables are already set to 0 or 1), we select one of $\mathbf{q}$ variables for partitioning. In particular, for the relaxation solution $\hat{\psi}_z$, the relaxation error of a discrete variable q_{ij}^m is $\min\{\hat{q}_{ij}^m - \lfloor \hat{q}_{ij}^m \rfloor, \lfloor \hat{q}_{ij}^m \rfloor + 1 - \hat{q}_{ij}^m\}$, where $\hat{q}_{ij}^m$ is the value of variable q_{ij}^m in solution $\hat{\psi}_z$. Assuming the value set of q_{ij}^m in Problem z is $\{q_0, q_1, \ldots, q_K\}$, its value set in Problems z_1 and z_2 will be $\{q_0, q_1, \ldots, \lfloor \hat{q}_{ij}^m \rfloor\}$ and $\{\lfloor \hat{q}_{ij}^m \rfloor + 1, \lfloor \hat{q}_{ij}^m \rfloor + 2, \ldots, q_K\}$, respectively. Again, we may pose more limitations on other variables based on the new value set of q_{ij}^m. In particular, if q_{ij}^m is 0, then we have $x_{ij}^m = 0$ based on Equation (12.22). If the new value set of q_{ij}^m does not include 0, then we have $x_{ij}^m = 1$ based on Equation (12.19).

Note that when all possible partition variables in $\mathbf{x}$ and $\mathbf{q}$ can no longer be partitioned (i.e., all values are assigned), the other variables can be solved via a linear program (LP).

12.4 NUMERICAL RESULTS FOR THE THROUGHPUT MAXIMIZATION PROBLEM

In this section, we present some numerical results for the case study in Section 12.3. The purpose of this effort is to offer quantitative understanding on the joint optimization at different layers.

12.4.1 Simulation Setting

For ease of exposition, we normalize all units for distance, bandwidth, rate, and power based on Equation (12.17) with appropriate dimensions. We consider 20-, 30-, and 50-node CR networks with each node randomly located in a 50×50 area (see later Figures 12.8, 12.10, and 12.12). We assume there are $|\mathcal{M}| = 10$ frequency bands in the network and each band has a bandwidth of $W = 50$. At each CR node, only a subset of these bands is available. For the 20- and 30-node networks, we assume there are five user communication sessions, with source node and destination node randomly selected and the minimum rate requirement of each session randomly generated within [1, 10] (see later Tables 12.4 and 12.6). For the 50-node network, the number of user communication sessions is 10 (see later Table 12.8).

We assume that the propagation gain model is $g_{ij} = d_{ij}^{-4}$ and the SINR threshold is $\alpha = 3$ [543]. The maximum transmission power at each node is $P_{\max} = 4.8 \cdot 10^5$ mW. We assume that the number of power control levels is $Q = 10$.

For our proposed branch-and-bound solution procedure, we set ε to 0.1, which guarantees that the obtained solution is 90% optimal.

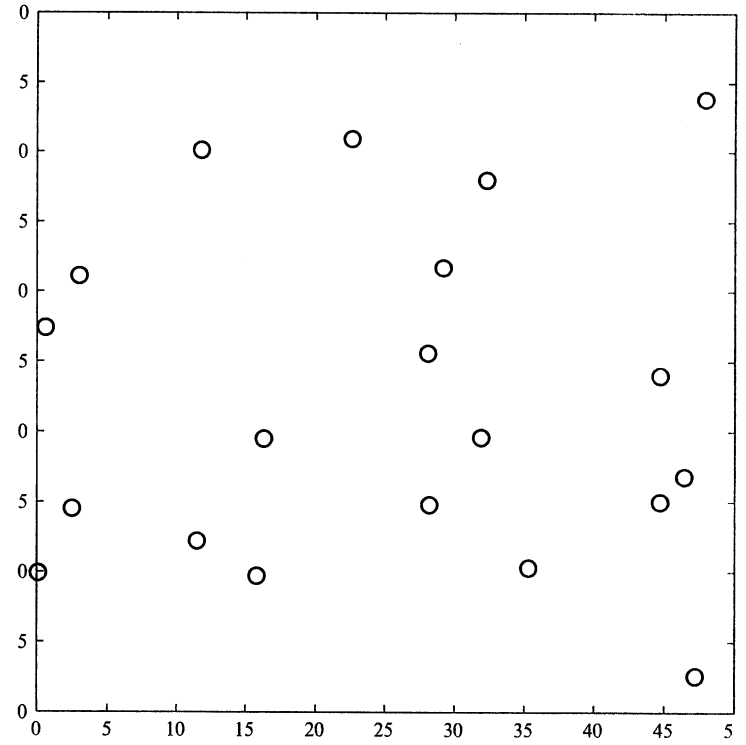

FIGURE 12.8

A 20-node network.

12.4.2 Results and Observations

A 20-Node Network

For the 20-node network in Figure 12.8, the location and available bands at each node are given in Table 12.3. There are five sessions. The source node, destination node, and minimum rate requirement of each session are shown in Table 12.4. The transmission power levels on their respective frequency bands in the final solution are:

Band 1: $q_{7,3}^1 = 1, q_{16,12}^1 = 7$
Band 2: $q_{8,2}^2 = 2$
Band 3: $q_{13,14}^3 = 2$
Band 4: $q_{1,7}^4 = 7, q_{2,10}^4 = 2$
Band 5: $q_{11,10}^5 = 1$
Band 6: $q_{15,19}^6 = 9$

Table 12.3 Location and Available Frequency Bands at Each Node for a 20-Node Network

Node	Location	Available Bands	Node	Location	Available Bands
1	(0.1, 9.9)	1, 2, 3, 4, 7, 8, 9, 10	11	(28.1, 25.6)	1, 2, 3, 4, 5, 6, 7, 8, 9, 10
2	(29.2, 31.7)	1, 2, 3, 4, 5, 7, 8, 10	12	(32.3, 38)	1, 8, 9, 10
3	(3, 31.1)	1, 4, 5, 6	13	(47.2, 2.6)	3, 5, 10
4	(11.8, 40.1)	1, 2, 3, 4, 6, 9, 10	14	(44.7, 15)	2, 3, 6, 7, 8
5	(15.8, 9.7)	1, 2, 3, 5, 6, 8, 9	15	(44.7, 24)	1, 2, 3, 4, 5, 6, 7, 8, 9, 10
6	(16.3, 19.5)	3, 5, 6, 8, 9	16	(47.9, 43.8)	1, 3
7	(0.6, 27.4)	1, 4, 8, 9, 10	17	(46.4, 16.8)	1, 7, 9
8	(22.6, 40.9)	1, 2, 3, 5, 7, 9, 10	18	(11.5, 12.2)	2, 5, 6, 10
9	(35.3, 10.3)	2, 9	19	(28.2, 14.8)	4, 5, 6, 7, 8, 9, 10
10	(31.9, 19.6)	1, 2, 3, 4, 5, 6, 7, 8, 9, 10	20	(2.5, 14.5)	1, 7, 10

Table 12.4 Source Node, Destination Node, and Minimum Rate Requirement of Each Session in the 20-Node Network

Session l	Source Node $s(l)$	Dest. Node $d(l)$	Min Rate Req. $r(l)$
1	16	10	9
2	18	3	1
3	12	11	4
4	13	17	3
5	15	6	2

Band 7: $q^7_{14,17} = 1$, $q^7_{20,1} = 1$
Band 8: $q^8_{12,11} = 3$
Band 9: $q^9_{12,8} = 1$, $q^9_{19,6} = 3$
Band 10: $q^{10}_{18,20} = 1$

Note that the same frequency band may be used by concurrent transmissions; for example, both node 7 (to 3) and node 16 (to 12) are transmitting on band 1. To minimize interference, our solution places these concurrent transmissions sufficiently apart and sets the optimal transmission power less than the maximum.

Figure 12.9 shows the flow routing topology in the final solution. The flow rates are:

Session 1: $f_{2,10}(1) = 103.30$, $f_{8,2}(1) = 103.30$, $f_{11,10}(1) = 15.86$, $f_{12,8}(1) = 103.30, f_{12,11}(1) = 15.86, f_{16,12}(1) = 119.16$
Session 2: $f_{1,7}(2) = 13.24, f_{7,3}(2) = 13.24, f_{18,20}(2) = 13.24, f_{20,1}(2) = 13.24$
Session 3: $f_{12,11}(3) = 52.96$

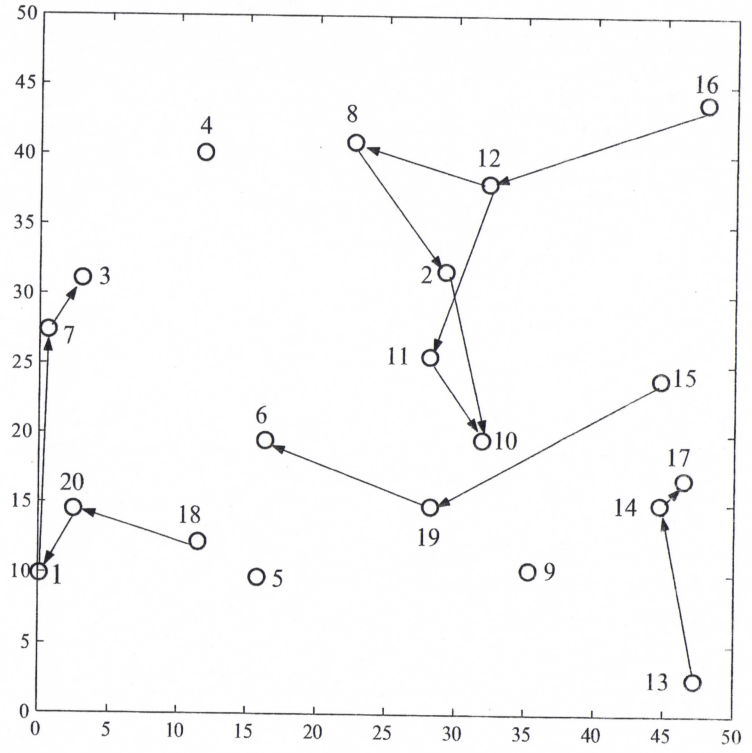

FIGURE 12.9

The flow routing topology in the final solution for the 20-node network.

Session 4: $f_{13,14}(4) = 39.72, f_{14,17}(4) = 39.72$
Session 5: $f_{15,19}(5) = 26.48, f_{19,6}(5) = 26.48$

We can see that, to maximize the achieved capacity, multipath routing is used (e.g., for session 1).

Under this solution, the achieved data rates for sessions 1 to 5 are 119.16, 13.24, 52.96, 39.72, and 26.48, respectively, and the achieved rate scaling factor is 13.24.

A 30-Node Network

For the 30-node network in Figure 12.10, the location and available bands at each node are given in Table 12.5. There are five sessions. The source node, destination node, and minimum rate requirement of each session are shown in Table 12.6. The transmission power levels on their respective frequency bands in the final solution are

Band 1: $q^1_{4,1} = 1, q^1_{21,28} = 1$
Band 2: $q^2_{28,13} = 3$
Band 3: $q^3_{19,29} = 9$
Band 4: $q^4_{23,29} = 4$
Band 5: $q^5_{26,29} = 1$
Band 6: $q^6_{13,11} = 2$
Band 7: $q^7_{16,21} = 4$
Band 8: $q^8_{16,13} = 2$
Band 9: $q^9_{26,22} = 7$
Band 11: $q^{11}_{17,16} = 2$
Band 12: $q^{12}_{19,23} = 1$
Band 14: $q^{14}_{22,15} = 1$

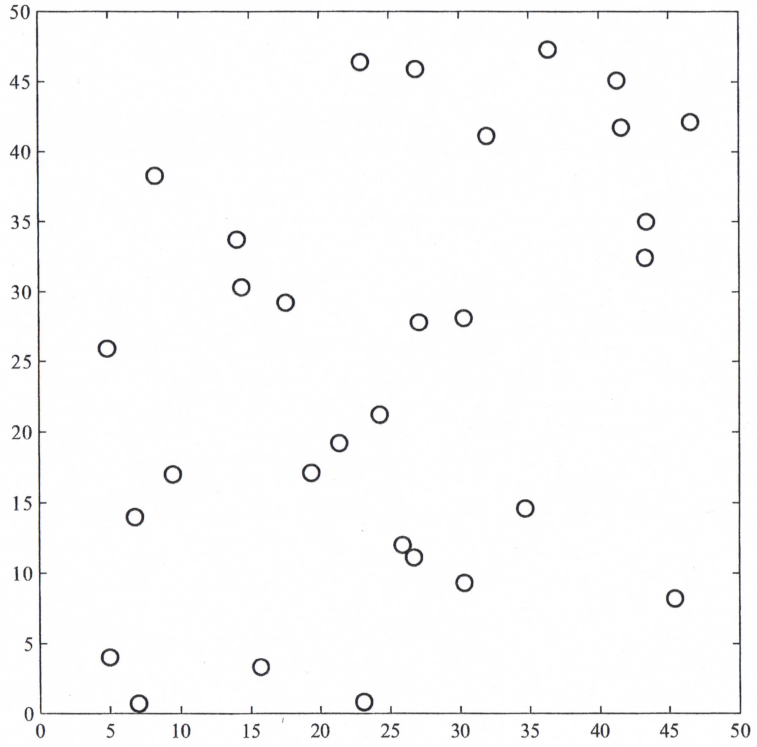

FIGURE 12.10

A 30-node network.

Table 12.5 Location and Available Frequency Bands at Each Node for a 30-Node Network

Node	Location	Available Bands	Node	Location	Available Bands
1	(7, 0.7)	1, 2, 6, 7, 16, 17, 19, 20	16	(30.3, 28.1)	7, 8, 11, 16, 17, 19, 20
2	(5, 4)	3, 5, 9, 12, 14, 15	17	(32, 41.1)	7, 11, 16, 17, 19, 20
3	(6.8, 14)	1, 2, 6, 7, 8, 11, 16, 17, 19, 20	18	(14.1, 33.7)	3, 4, 5
4	(15.7, 3.3)	1, 2, 7, 16, 20	19	(23, 46.4)	3, 12, 15
5	(9.5, 17)	3, 4, 5, 9, 12	20	(30.3, 9.3)	5, 9
6	(19.4, 17.1)	1, 2, 6, 7, 8, 16, 19, 20	21	(17.6, 29.2)	1, 2, 6, 7, 8, 11, 16, 17, 19, 20
7	(34.7, 14.6)	3, 4, 5, 9, 12, 14	22	(27.1, 27.8)	9, 12, 14, 15
8	(4.9, 25.9)	3, 4, 12	23	(26.9, 45.9)	3, 4, 5, 9, 10, 12, 13, 14, 15, 17
9	(46.6, 42.1)	10, 18	24	(43.3, 32.4)	1, 2, 11, 16, 17, 20
10	(8.3, 38.3)	3, 4, 5, 9, 14	25	(45.4, 8.2)	3, 4, 5, 9, 12, 14
11	(26.7, 11.1)	1, 6, 7, 8, 11, 16, 17, 19, 20	26	(43.4, 35)	3, 5, 9, 15
12	(36.4, 47.3)	10, 13, 18	27	(41.3, 45.1)	1, 16, 20
13	(24.3, 21.2)	1, 2, 6, 8, 11, 19	28	(14.4, 30.3)	1, 2, 6, 7, 8, 11, 16, 17, 20
14	(23.1, 0.8)	3, 5, 9, 14	29	(41.6, 41.7)	3, 4, 5, 9, 10, 12, 14, 15, 18
15	(21.4, 19.2)	4, 9, 12, 14	30	(25.9, 12)	1, 2, 6, 7, 8, 11, 16, 17, 19, 20

Table 12.6 Source Node, Destination Node, and Minimum Rate Requirement of Each Session in the 30-Node Network

Session l	Source Node $s(l)$	Dest. Node $d(l)$	Min Rate Req. $r(l)$
1	16	28	4
2	24	11	7
3	13	1	1
4	19	29	8
5	26	15	1

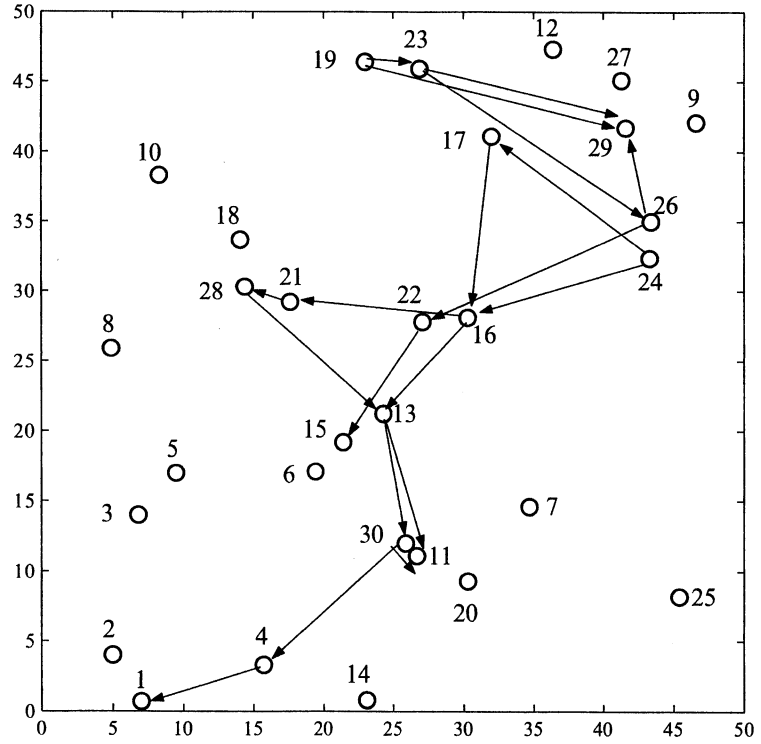

FIGURE 12.11

The flow routing topology in the final solution for the 30-node network.

Band 15: $q_{23,26}^{15} = 10$
Band 16: $q_{24,17}^{16} = 3, q_{30,11}^{16} = 1$
Band 17: $q_{24,16}^{17} = 7$
Band 19: $q_{13,30}^{19} = 1$
Band 20: $q_{30,4}^{20} = 4$

Note that the same frequency band may be used by concurrent transmissions; for example, both node 4 (to 1) and node 21 (to 28) are transmitting on band 1. To minimize interference, our solution places these concurrent transmissions sufficiently apart and sets the optimal transmission power less than the maximum.

Figure 12.11 shows the flow routing topology in the final solution.

Session 1: $f_{16,21}(1) = 124.72, f_{21,28}(1) = 124.72$
Session 2: $f_{13,11}(2) = 160.58$, $f_{13,30}(2) = 57.68$, $f_{16,21}(2) = 24.22$, $f_{16,13}(2) = 194.04$, $f_{17,16}(2) = 104.36$, $f_{21,28}(2) = 24.22$, $f_{24,16}(2) = 113.90$, $f_{24,17}(2) = 104.36, f_{28,13}(2) = 24.22, f_{30,11}(2) = 57.68$
Session 3: $f_{13,30}(4) = 31.18, f_{30,4}(3) = 31.18, f_{4,1}(3) = 31.18$
Session 4: $f_{19,23}(4) = 211.19, f_{19,29}(4) = 103.33, f_{23,26}(4) = 102.46, f_{23,29}(4) = 108.73, f_{26,29}(4) = 102.46$
Session 5: $f_{22,15}(5) = 39.32, f_{26,22}(5) = 39.32$

We can see that, to maximize the achieved capacity, multipath routing is used (e.g., for session 2).

Under this solution, the achieved data rates for sessions 1 to 5 are 124.72, 218.26, 31.18, 314.52, and 39.32, respectively, and the achieved rate scaling factor is 31.18.

A 50-Node Network

For the 50-node network in Figure 12.12, the location and available bands at each node are given in Table 12.7. There are 10 sessions. The source node, destination

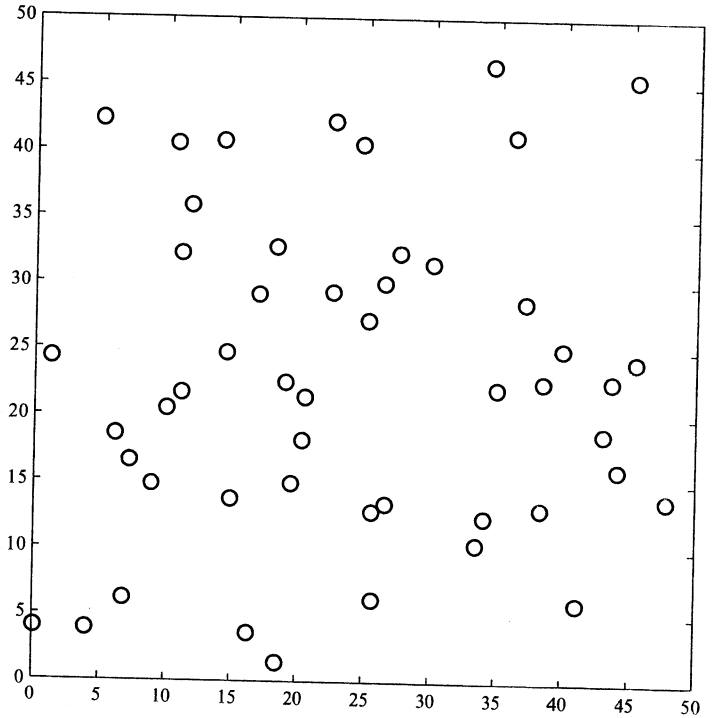

FIGURE 12.12

A 50-node network.

Table 12.7 Location and Available Frequency Bands at Each Node for a 50-Node Network

Node	Location	Available Bands	Node	Location	Available Bands
1	(11.1, 21.7)	2, 3, 4, 8, 25	26	(25.2, 27.2)	10, 14, 20, 24, 26
2	(0.1, 4)	6, 7, 10, 13, 14, 20, 23, 24, 26, 28	27	(22.5, 42.2)	5, 9, 12, 16, 18, 27, 29, 30
3	(7.2, 16.6)	6, 10, 14, 20, 23, 24, 26	28	(30, 31.5)	6, 13, 24, 26, 28
4	(11, 32.2)	6, 7, 10, 13, 14, 20, 23, 24, 26, 28	29	(35, 22.1)	6, 10
5	(16.3, 3.6)	10, 13, 14, 20, 23	30	(25.7, 6.2)	5, 9, 12, 17, 18, 22, 27, 29, 30
6	(14.5, 24.7)	8, 11, 25	31	(34.1, 12.4)	9, 12, 16, 17, 30
7	(14.9, 13.7)	5, 9, 12, 16, 17, 18, 22, 27, 29, 30	32	(26.4, 30)	5, 9, 12, 16, 17, 18, 22, 27, 29, 30
8	(19.5, 14.9)	7, 24, 28	33	(14.1, 40.7)	1, 2, 25
9	(26.6, 13.4)	1, 19, 21, 25	34	(34.4, 46.5)	9, 17, 18, 30
10	(22.5, 29.3)	1, 3, 4, 8, 11, 15, 19	35	(19, 22.5)	1, 6, 7, 10, 13, 14, 20, 23, 24, 28
11	(24.6, 40.5)	3, 8, 25	36	(39.9, 25.1)	6, 13, 14, 20, 23, 24, 26, 28
12	(38.4, 13.1)	2, 8, 11, 15	37	(20.3, 18.2)	1, 2, 3, 4, 8, 11, 15, 19, 21, 27
13	(4, 3.9)	9, 12, 16, 22, 27, 29, 30	38	(10, 20.5)	6, 7, 10, 13, 14, 20, 23, 24, 26, 28
14	(6.1, 18.6)	9, 12, 16, 17, 18, 22, 27, 30	39	(20.5, 21.4)	1, 2, 3, 4, 8, 11, 15, 19, 21, 25
15	(38.5, 22.6)	2, 4, 11, 15, 19, 21, 25	40	(37.1, 28.6)	7, 10, 13, 14, 20, 23, 24, 26
16	(1.2, 24.3)	5, 9, 12, 17, 22, 29, 30	41	(44.1, 16.1)	1, 15, 21
17	(4.9, 42.3)	5, 27	42	(41.1, 6)	9, 29
18	(18.5, 1.4)	5, 9, 12, 17, 18, 27, 30	43	(43, 18.8)	5, 9, 12, 16, 18, 22
19	(16.9, 29.1)	3, 4, 10, 11, 12, 15	44	(45.4, 24.2)	9, 12, 16, 17, 18, 30
20	(33.5, 10.4)	7, 13, 14, 20, 23, 24, 26, 28	45	(36.2, 41.2)	5, 9, 17, 27, 29, 30
21	(25.6, 12.8)	6, 7, 20, 23, 24, 28	46	(27.5, 32.3)	12, 16, 17, 18, 29, 30
22	(45.2, 45.5)	2, 8, 15, 19	47	(47.8, 13.8)	22, 27, 29, 30
23	(43.6, 22.7)	1, 2, 3, 4, 11, 15, 19, 21	48	(8.9, 14.8)	5, 30
24	(10.6, 40.5)	4, 15, 19, 21, 25	49	(6.8, 6.2)	5, 9, 12, 16, 17, 27, 30
25	(18.2, 32.7)	9, 12, 18, 22, 27	50	(11.7, 35.8)	1, 2, 3, 4, 8, 11, 15, 19, 21, 25

Table 12.8 Source Node, Destination Node, and Minimum Rate Requirement of Each Session in the 50-Node Network

Session l	Source Node $s(l)$	Dest. Node $d(l)$	Min Rate Req. $r(l)$
1	21	4	4
2	5	26	7
3	19	20	6
4	33	6	10
5	37	10	9
6	23	11	2
7	25	46	3
8	42	43	9
9	44	27	8
10	47	30	1

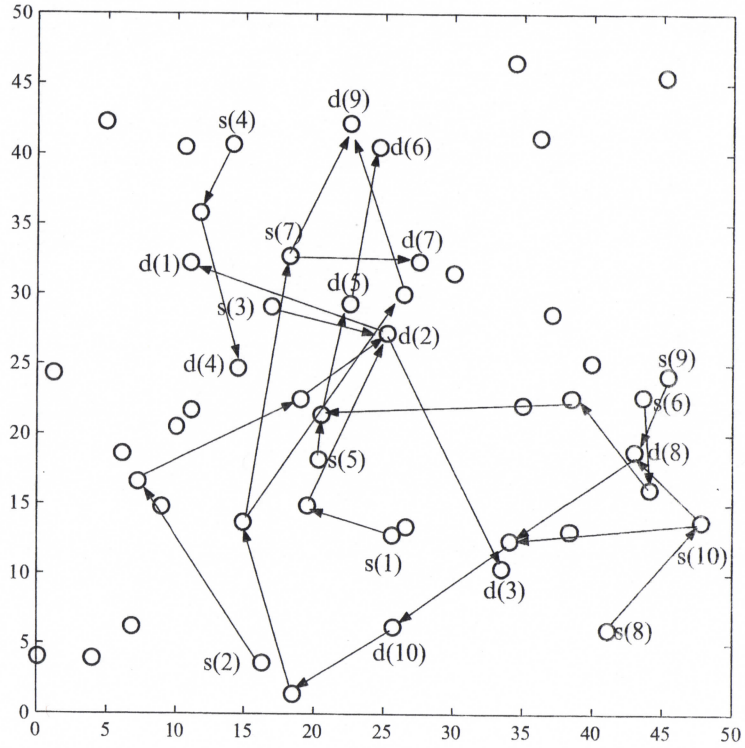

FIGURE 12.13

The flow routing topology in the final solution for the 50-node network.

node, and minimum rate requirement of each session are shown in Table 12.8. The routing topology is shown in Figure 12.13. The detailed transmission power levels and flow rates in this solution are omitted to conserve space. We can see that it is necessary to employ multipath routing for sessions 9 and 10. The scaling factor in the final solution is 13.36.

12.5 CHAPTER SUMMARY

In this chapter, we study cross-layer optimization for multihop CR networks. We give joint consideration of power control at the physical layer, scheduling at the link layer, and flow routing at the network layer. We present mathematical models to characterize the interdependency among power control, scheduling, and routing. Our models are general and can be applied to many cross-layer optimization problems for multihop CR networks. As a case study, we apply our models to a throughput maximization problem for a multihop CR network. We develop a centralized solution procedure for this optimization problem based on a branch-and-bound framework. Using numerical results, we offer quantitative understanding on the joint optimization at different layers.

12.6 PROBLEMS

1 Compare CR and MC-MR wireless networks.

2 Discuss the impact of power control on scheduling and flow routing.

3 Consider a CR network where each node uses peak transmission power $P_{\max}$ (i.e., no power control).
   (a) Formulate the constraints for scheduling and successful transmission.
   (b) Comparing solutions with and without power control, which provides better performance (larger scaling factor)? Explain.

4 Discuss the impact of scheduling on power control and flow routing.

5 Discuss the impact of flow routing on power control and scheduling.

6 Suppose flow splitting and multipath routing are not allowed.
   (a) What are the routing constraints?
   (b) Compare the single-path solutions and the multipath solutions and explain which achieve better performance.

7 Suppose the objective is to maximize the total data rate utility for all user sessions, where utility is $u(l) = \ln r(l)$ for session l. Write down the problem formulation in this case.

8 The problem considered in this chapter aims to maximize an objective. The branch-and-bound procedure to solve this problem is shown in Figure 12.5. For another problem that aims to minimize an objective, can we use the same branch-and-bound procedure? If not, how should we change the procedure to solve a minimization problem?

9 Why do we need linear relaxation in the branch-and-bound procedure?

10 Why do we need a local search in the branch-and-bound procedure?

11 When we select a partition variable, why should we select an x variable even if the relaxation error caused by this variable is less than that by a q variable?

12 After we obtain the values for all x and q variables, how do we solve the optimal values for other variables?

13 By a branch-and-bound procedure, can we get an optimal solution for the problem considered in this chapter? If yes, how should we change the procedure in Figure 12.5? Discuss the pros and cons to get an optimal solution and a $(1 - \varepsilon)$-optimal solution.